Alkane Oxidation by VO_2^+ in the Gas Phase: A Unique Dependence of Reactivity on the Chain Length

Marianne Engeser, Maria Schlangen, Detlef Schröder,* and Helmut Schwarz*

Institut für Chemie der Technischen Universität Berlin, Strasse des 17. Juni 135, D-10623 Berlin, Germany

Takashi Yumura and Kazunari Yoshizawa*

Institute for Fundamental Research of Organic Chemistry, Kyushu University, Fukuoka 812-8581, Japan

Received May 12, 2003

The oxidation of small alkanes by the vanadium oxide cation VO_2^+ in the gas phase has been studied by Fourier transform ion-cyclotron resonance mass spectrometry (FTICR-MS). Sophisticated mass spectrometric experiments in conjunction with investigation of deuterium-labeled substances are used to elucidate the mechanistic details of the reactions. In marked contrast to oxidative dehydrogenation followed by elimination of ethene in the reaction of VO_2^+ with ethane, the corresponding reaction with propane mainly affords elimination of dihydrogen concomitant with an ionic product assigned to the allyl complex $(\eta^3\text{-}C_3H_5)V(O)(OH)^+$. In the case of *n*-butane/VO_2^+, a combined loss of H_2 and H_2O provides yet another product channel. Branching ratios, reaction rates, and some mechanistic aspects of the oxidation of propane, *n*-butane, and isobutane by VO_2^+ are reported. The experiments are complemented by a computational study of the potential energy surface of propane/VO_2^+ by means of density functional theory.

Introduction

Vanadium oxides are among the most important transition metal catalysts used in the chemical industry today. Besides other applications, selective oxidation of propane and butane can be achieved using vanadium oxides and related compounds.[1,2] Yet, it remains a major goal to develop a basic understanding of the very complex mechanisms involved on a molecular level. In the economically relevant oxidation of butane to maleic anhydride on vanadium oxide catalysts, for example, it is still under debate whether the various oxygen and hydrogen transfers all take place at a single reactive site or whether several different reaction centers on the surface are needed.[3] Elucidation of the role of isolated vanadium−oxygen units in heterogeneous catalysis can be aided by gas-phase studies, which can provide insight into the intrinsic properties and reactivities of discrete and well-characterized species.

The reactions of the simplest cationic vanadium oxide VO^+ with alkanes are similar to those of the bare metal cation V^+, except for a markedly decreased reactivity of VO^+ compared to the V^+ cation.[4] Likewise, mere associations prevail in the reactions of alkanes with vanadium oxide clusters having high oxygen/vanadium ratios.[5−7] These similarities are contrasted by the efficient oxidative dehydrogenation of ethane by the vanadium dioxide cation in the gas phase.[8]

Here, we report the reactions of the vanadium dioxide cation VO_2^+ with propane and the isomeric butanes. In addition to the experimental studies, the potential energy surface of the reaction of VO_2^+ with propane is investigated by means of density functional theory.

Experimental Methods

Ion/molecule reactions are examined with a Spectrospin CMS 47X FTICR mass spectrometer equipped with an external ion source as described elsewhere.[9,10] In brief, V^+ is generated by laser ablation of a vanadium target using a Nd:YAG laser operating at 1064 nm. A series of potentials and ion lenses is used to transfer the ions to the ICR cell, which is positioned in the bore of a 7.05 T superconducting magnet. All mass selections are performed using the FERETS protocol,[11] a computer-controlled routine that combines frequency sweeps and single frequency shots to optimize ion isolation. Mass-selected $^{51}V^+$ is then converted to VO_2^+ by reaction with pulsed-

(1) Centi, G.; Cavani, F.; Trifiro, F. *Selective Oxidation by Heterogeneous Catalysis*; Kluwer Academic/Plenum Publishers: New York, 2001.
(2) For a whole issue dedicated exclusively to this topic, see: *Appl. Catal. A* **1997**, *157*.
(3) Chen, B.; Munson, E. J. *J. Am. Chem. Soc.* **2002**, *124*, 1638−1652.
(4) Jackson, T. C.; Carlin, T. J.; Freiser, B. S. *J. Am. Chem. Soc.* **1986**, *108*, 1120−1126.
(5) Bell, R. C.; Zemski, K. A.; Kerns, K. P.; Deng, H. T.; Castleman, A. W. *J. Phys. Chem. A* **1998**, *102*, 1733−1742.
(6) Zemski, K. A.; Justes, D. R.; Castleman, A. W. *J. Phys. Chem. A* **2001**, *105*, 10237−10245.
(7) Schröder, D.; Engeser, M.; Brönstrup, M.; Daniel, C.; Spandl, J.; Hartl, H. *Int. J. Mass Spectrom.*, in press.
(8) Harvey, J. N.; Diefenbach, M.; Schröder, D.; Schwarz, H. *Int. J. Mass Spectrom.* **1999**, *182/183*, 85−97.
(9) Eller, K.; Schwarz, H. *Int. J. Mass Spectrom. Ion Processes* **1989**, *93*, 243−257.
(10) Engeser, M.; Schröder, D.; Weiske, T.; Schwarz H. *J. Phys. Chem. A* **2003**, *107*, 2855−2859.
(11) Forbes, R. A.; Laukien, F. H.; Wronka, J. *Int. J. Mass Spectrom. Ion Processes* **1988**, *83*, 23.

10.1021/om030353h CCC: $25.00
Publication on Web 08/16/2003

in N_2O; $VO_2H_2^+$ is generated by reacting ethane with mass-selected VO_2^+.[8] During the gas pulses, the ions undergo hundreds of collisions such that the product ions are assumed to be equilibrated to ambient temperature (298 K).[12] The reactivities of the mass-selected ions of interest are studied by introducing neutral reactants via leak valves at stationary pressures on the order of 10^{-8} mbar. The experimental second-order rate constants are evaluated assuming the pseudo-first-order kinetic approximation after calibration of the measured pressures and acknowledgment of the ion gauge sensitivities.[13] The error of the absolute rate constants is ±30%, whereas the error for the relative rate constants is only 10%. Branching ratios and rate constants are derived from the analysis of the reaction kinetics and are reported within an error of ±25%. Within experimental error, all primary reactions described below show strict pseudo-first-order behavior, thus supporting the assumed equilibration of the ions to 298 K. In addition, the reactivities of the major product ions formed in the experiments are monitored after mass selection as described above. In some consecutive reactions, the observed time dependencies of the product distributions are interpreted by means of kinetic modeling.[14] The first-order kinetics of the reacting ions provide the rate constants k_{exp}, which are compared to the gas-kinetic collision rates k_c[15] in terms of efficiencies ϕ. Further, several ions are characterized by collision-induced dissociation[16,17] (CID) brought about by excitation of the mass-selected ions using an rf-pulse in the presence of argon gas with pressures on the order of 10^{-7} mbar.

All unlabeled reagents, [2,2-D_2]-propane, [D_8]-propane, and [1,1,1-D_3]-butane were used as purchased and introduced into the ICR by conventional vacuum techniques. The other labeled alkanes were prepared by hydrolysis of the corresponding Grignard reagents and purified using standard laboratory procedures.

Theoretical Methods

All calculations employ the hybrid density functional theory (DFT) method B3LYP[18−21] as implemented in the Gaussian 98 program.[22] This method comprises Slater exchange, Hartree−Fock exchange, the exchange functional of Becke,[18] the correlation functional of Lee, Yang, and Parr (LYP),[19] and the correlation functional of Vosco, Wilk, and Nusair.[23] The contribution of each energy to the B3LYP energy expression was empirically fitted by the procedure of Becke[18] on a reference set of molecules. This hybrid DFT method has been reported to provide excellent descriptions of various reaction profiles, particularly with respect to geometries, heats of reaction, barrier heights, and molecular vibrations.[24] For the V atom, the (14s9p5d) primitive set of Wachters[25] is applied supplemented with one polarization f-function ($\alpha = 0.78$), resulting in a (611111111|51111|311|1) [9s5p3d1f] contraction;[26] H, C, and O are treated with 6-311G** basis sets.[27] Vibrational frequencies are computed for all stationary points obtained in order to confirm that each optimized geometry corresponds to a local minimum (no imaginary frequency) or to a saddle point (only one imaginary frequency). All energies given below refer to 0 K including zero-point energy correction.

Experimental Results

As reported previously, ethane reacts with VO_2^+ to yield the $VO_2H_2^+$ cation concomitant with ethene being formed as a neutral molecule.[8] Overall, this reaction corresponds to an oxidative dehydrogenation of the alkane associated with a reduction from formal V^V in the reactant ion VO_2^+ to V^{III} in the ionic product $VO_2H_2^+$, i.e., either the metal dihydroxide $V(OH)_2^+$ or the hydrated metal oxide $OV(OH_2)^+$.[28] The present work describes an extension to the reactions of VO_2^+ with larger alkanes, where some unexpected changes of the reactivity patterns are observed as summarized in Figure 1.

Upon reacting mass-selected VO_2^+ with propane, it turns out quite surprisingly that losses of one or even two molecules of dihydrogen prevail. Compared to the reaction of C_2H_6 with VO_2^+, the reaction rate of propane is about 4 times larger. The product pattern changes once more for the next member of the homologous row, in that butane reacts with VO_2^+ in yet a different manner. Apart from 15% loss of C_4H_8, which resembles the loss of ethene in the ethane/VO_2^+ system, four new reaction channels appear for butane/VO_2^+. Thus, instead of a simple elimination of H_2 like in the propane/VO_2^+ system, 31% of a combined loss of H_2 and H_2O is observed. Furthermore, C−C bond cleavages lead to losses of the neutral C_1 and C_2 fragments methane and ethene, respectively, but interestingly not ethane. Finally, the reactivity of isobutane with VO_2^+ shows some features of both the propane/VO_2^+ system (H_2 elimination) and the butane/VO_2^+ system (H_2/H_2O elimination). Not surprisingly, methane elimination is much more pronounced in the isobutane/VO_2^+ system than in *n*-butane/VO_2^+. The major product of the isobutane/VO_2^+ system corresponds to the carbenium ion $C_4H_9^+$, however, which is once more unique to this particular alkane.

The marked switches in reactivity from ethane to propane and then to butane and isobutane are unexpected and have no precedents in the gas-phase chemistry of alkanes with transition metal ions.[29] Usually,

(12) Schröder, D.; Schwarz, H.; Clemmer, D. E.; Chen, Y.-M.; Armentrout, P. B.; Baranov, V. I.; Böhme, D. K. *Int. J. Mass Spectrom. Ion Processes* **1997**, *161*, 175−191.
(13) Bartmess, J. E.; Georgiadis, R. M. *Vacuum* **1983**, *33*, 149−156.
(14) Brown, J. R.; Schwerdtfeger, P.; Schröder, D.; Schwarz, H. *J. Am. Soc. Mass Spectrom.* **2002**, *13*, 485−492.
(15) Su, T. *J. Chem. Phys.* **1988**, *89*, 5355, and references therein.
(16) Burnier, R. C.; Cody, R. B.; Freiser, B. S. *J. Am. Chem. Soc.* **1982**, *104*, 7436−7441.
(17) Cody, R. B.; Freiser, B. S. *Int. J. Mass Spectrom. Ion Phys.* **1982**, *41*, 199−204.
(18) Becke, A. D. *Phys. Rev. A* **1988**, *38*, 3098−3100.
(19) Becke, A. D. *J. Chem. Phys.* **1993**, *98*, 5648−5652.
(20) Stephens, P. J.; Devlin, F. J.; Chabalowski, C. F.; Frisch, M. J. *J. Phys. Chem.* **1994**, *98*, 11623−11627.
(21) Lee, C.; Yang, W.; Parr, R. G. *Phys. Rev. B* **1988**, *37*, 785−789.
(22) Frisch, M. J.; Trucks, G. W.; Schlegel, H. B.; Scuseria, G. E.; Robb, M. A.; Cheeseman, J. R.; Zakrzewski, V. G.; Montgomery, J. A.; Stratmann, R. E.; Burant, J. C.; Dapprich, S.; Millam, J. M.; Daniels, A. D.; Kudin, K. N.; Strain, M. C.; Farkas, O.; Tomasi, J.; Barone, V.; Cossi, M.; Cammi, R.; Mennucci, B.; Pomelli, C.; Adamo, C.; Clifford, S.; Ochterski, J.; Petersson, G. A.; Ayala, P. Y.; Cui, Q.; Morokuma, K.; Malick, D. K.; Rabuck, A. D.; Raghavachari, K.; Foresman, J. B.; Cioslowski, J.; Ortiz, J. V.; Stefanov, B. B.; Liu, G.; Liashenko, A.; Piskorz, P.; Komaromi, I.; Gomperts, R.; Martin, R. L.; Fox, D. J.; Keith, T.; Al-Laham, M. A.; Peng, C. Y.; Nanayakkara, A.; Gonzalez, C.; Challacombe, M.; Gill, P. M. W.; Johnson, B. G.; Chen, W.; Wong, M. W.; Andres, J. L.; Head-Gordon, M.; Replogle, E. S.; Pople, J. A. *Gaussian 98*; Gaussian Inc.: Pittsburgh, PA, 1998.
(23) Vosko, S. H.; Wilk, L.; Nusair, M. *Can. J. Phys.* **1980**, *58*, 1200−1211.
(24) Baker, J.; Muir, M.; Andzelm, J.; Scheiner, A. In *Chemical Applications of Density-Functional Theory*; Laird, B. B., Ross, R. B., Ziegler, T., Eds.; ACS Symposium Series 629; American Chemical Society: Washington, DC, 1996.
(25) Wachters, A. J. H. *J. Chem. Phys.* **1970**, *52*, 1033−1036.
(26) Raghavachari, K.; Trucks, G. W. *J. Chem. Phys.* **1989**, *91* 1062−1065.
(27) Raghavachari, K.; Binkley, J. S.; Seeger, R.; Pople, J. A. *J. Chem. Phys.* **1980**, *72*, 650−654.
(28) Koyanagi, G. K.; Bohme, D. K.; Kretzschmar, I.; Schröder, D.; Schwarz, H. *J. Phys. Chem. A* **2001**, *105*, 4259−4270.
(29) Eller, K.; Schwarz, H. *Chem. Rev.* **1991**, *91*, 1121−1177.

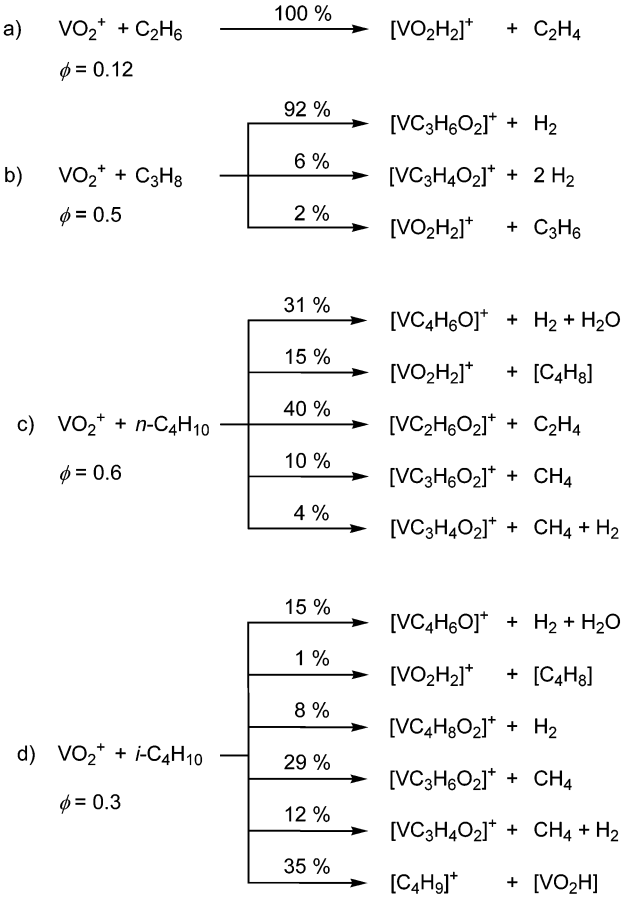

Figure 1. Reaction efficiencies (ϕ)[41] and primary product branching ratios for the reactions of VO_2^+ with small alkanes. The data for ethane are taken from ref 8.

the reactivities of cationic transition metals or the corresponding oxide cations toward alkanes scale with the size of the substrate. Thus, C−H and C−C bond activations commence to occur at a specific minimum chain length of the hydrocarbon and from there on are observed for the larger alkanes as well.[30] Bare V^+, for example, and the VO^+ monocation exhibit such a behavior.[4] Note that VO^+ is far less reactive than V^+ itself, indicating that the oxygen atom in VO^+ does not participate in the bond activations observed, but rather acts as a mere spectator ligand. In the following, the reactions of propane and the two butanes with thermalized VO_2^+ cations in the gas phase are discussed in more detail.

Propane/VO_2^+. As mentioned above, the major reaction of propane with VO_2^+ leads to dehydrogenation concomitant with formation of a $[VC_3H_6O_2]^+$ cation. Therefore, let us begin with more experiments aimed at elucidating the structure of this particular product ion. At room temperature, the mass-selected $[VC_3H_6O_2]^+$ ion generated from propane/VO_2^+ neither reacts any further with propane nor shows any reactivity toward additionally leaked-in benzene. Yet, one observes a slow addition of background water leading to $[VC_3H_8O_3]^+$ and subsequently $[VO_4H_4]^+$, where the latter is assigned to the exchange of a propene ligand with a second water molecule. From a mechanistic perspective, the observation of $[VO_4H_4]^+$ implies that the formal oxidation state V^V of the initial VO_2^+ cation is maintained throughout the entire reaction sequence $VO_2^+ \rightarrow [VC_3H_6O_2]^+ \rightarrow [VC_3H_8O_3]^+ \rightarrow [VO_4H_4]^+$ (or recovered in the final steps) because irrespective of the connectivity of $[VO_4H_4]^+$, i.e., either $V(OH)_4^+$, $OV(OH)_2(H_2O)^+$, or $VO_2(H_2O)_2^+$, the elemental composition as such suggests the oxidation state V^V. This finding is in sharp contrast to the reactions of VO_2^+ with ethane and butane, in which the products $V(OH)_2^+$ and $(C_4H_6)VO^+$, respectively, can clearly be assigned to V^{III}.

Table 1. Intensities[a] for the Loss of Dihydrogen from Propane Isotopologs upon Reaction with VO_2^+ (figures calculated for a completely random H/D distribution are given in italics)

	$-H_2$		$-HD$		$-D_2$	
$CH_3CH_2CH_3$	100	*100*				
CH_3CHDCH_3	73	*75*	27	*25*		
$CH_3CD_2CH_3$	50	*53*	47	*43*	3	*4*
$CD_3CH_2CH_3$	18	*36*	82	*53*	0	*11*
$CD_3CD_2CH_3$	0	*11*	67	*53*	33	*36*
$CD_3CH_2CD_3$	10	*4*	60	*43*	30	*53*
$CD_3CD_2CD_3$					100	*100*

[a] Observed intensities are ^{13}C-corrected, extrapolated to a reaction time of 0 s to account for H/D exchange with background water, and normalized to $\Sigma = 100$.

Further insight is achieved by consideration of the reactions of VO_2^+ with fully deuterated propane. Comparison of the reaction kinetics for $[D_0]$- and $[D_8]$-propane implies a negligible intermolecular kinetic isotope effect (KIE) as the rate constants coincide within experimental error (5.3×10^{-10} and 5.2×10^{-10} cm^3 $molecules^{-1}$ s^{-1}, respectively). Accordingly, C−H(D) bond activation of propane is not a major contributor to any possible overall KIE between propane and its fully deuterated variant. It would be misleading, however, to conclude that C−H(D) bond activation is not rate-determining because the intermolecular KIE is not a sensitive measure in this respect. In fact, Derrick and Donchi have stated that "intermolecular (kinetic isotope) effects can be effectively independent of transition state characteristics".[31] Interestingly, the corresponding $[VC_3D_6O_2]^+$ product ion ($m/z = 131$) undergoes sequential H/D exchange with water present in the background of the mass spectrometer. A fit of the time dependences of the observed relative intensities of the signals between $m/z = 125-131$ implies that the first H/D exchange is about 3 times faster than the following ones. Accordingly, one hydrogen atom in $[VC_3D_6O_2]^+$ is bound distinctly differently from the others. The fast exchange with water may be considered as an indication for the presence of a hydroxyl group (see below).

Next, the reactions of five partially deuterated propanes are considered. The intensities observed for the losses of $H_2/HD/D_2$ upon reaction with VO_2^+ correspond neither to some regiospecific dehydrogenation nor to a completely statistical distribution of H and D atoms (Table 1). However, none of several kinetic models tested (including those based on the calculated mechanism described further below) could fit the experimental data reasonably well as long as inverse H/D kinetic isotope effects are avoided. The difficulty is most obvious when

(30) Burnier, R. C.; Byrd, G. D.; Carlin, T. J.; Wiese, M. B.; Cody, R. B.; Freiser, B. S. *Lect. Notes Chem.* **1982**, *31*, 98−118.

(31) Derrick, P. J.; Donchi, K. F. In *Comprehensive Chemical Kinetics*; Bamford, C. H., Tipper, C. F. H., Eds.; Elsevier: New York, 1983; Vol. 24, pp 53−247.

Chart 1

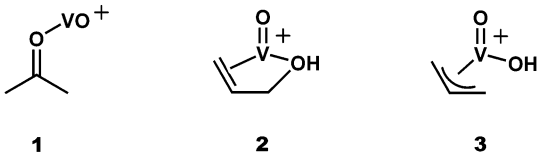

1 **2** **3**

the data for two isotopologs with inverted deuterium incorporation are compared, namely, [1,1,1-D_3]- and [1,1,1,2,2-D_5]-propane: the former loses only 18% of H_2, whereas loss of D_2 from the latter comprises 33%. The computational results reported further below hint toward some explanation of this seemingly erratic behavior in that the loss of dihydrogen from the propane/VO_2^+ system can by no means be considered as a direct process, but involves competitive activations of C−H bonds in all positions of propane concomitant with partial H/D equilibration. While we have recently demonstrated that even complicated isotope patterns can be kinetically modeled reasonably well provided that a sufficiently large set of appropriately labeled substrates is examined,[32−34] the reaction of VO_2^+ with propane appears too complex to apply a related procedure for the time being. Of course, the product distributions can be modeled, but these models either involve inverse KIEs, for whose operation we have no meaningful foundation, or require more assumptions than independent experimental parameters available. Irrespective of the failure to quantitatively model the observed intensities, several qualitative conclusions can be drawn from the experimental data presented in Table 1. At first, an entirely statistical H/D equilibration can be ruled out, because [1,1,1,2,2-D_5]-propane does not undergo loss of H_2, even though potential intramolecular KIEs should favor loss of the lighter isotopic variant. Further, as only loss of 100% HD should have been observed in the case of mere 1,2-elimination, the results of [2,2-D_2]-propane suggest a notable degree of a formal 1,3-dehydrogenation. This conclusion is further supported by the data for [2-D_1]-propane and the significant amount of D_2 formed from [1,1,1,3,3,3-D_6]-propane; note that a considerable intramolecular KIE might be operative in the latter case. The major problem in kinetic modeling is posed by [1,1,1-D_3]-propane, from which much more HD loss than anticipated is observed. This finding points to the occurrence of "hidden hydrogen transfers", that is, rate-determining C−H bond activations where the hydrogen atom of the initially activated C−H bond is not contained in the neutral molecules lost.[35] Such processes would indeed justify the involvement of formally inverse H/D isotope effects in the propene/VO_2^+ system as implied by the kinetic modelings mentioned above. However, any of these or other assumptions would immediately lead to an underdetermined system of differential equations such that the solutions lack chemical significance.

Further insight into the potential energy surface of the propane/VO_2^+ system can be obtained by attempts

Scheme 1

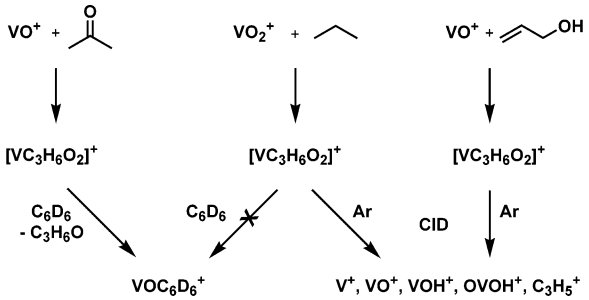

to independently generate $[VC_3H_6O_2]^+$ ions from different entrance channels. A viable approach is the reaction of VO^+ with *n*-propanol. Whereas the major channels afford loss of propene to form $VO_2H_2^+$ (77%) and formal hydroxide transfer to yield neutral VO_2H (15%), 5% of the ions lose H_2 to give rise to the desired product, and some amount of double dehydrogenation is observed (3%) as well. Two other $[VC_3H_6O_2]^+$ ions could be generated independently as described below. After the generation of VO^+, a pulse of acetone was used to form an ion $[VC_3H_6O_2]^+$, which most probably corresponds to the genuine (acetone)VO^+ complex (Chart 1, structure **1**), as the excess energy gained upon complexation can be lost in multiple collisions during the gas pulse. Subsequent mass selection of the product ion and reaction with perdeuterated benzene yields $(C_6D_6)VO^+$, which can be ascribed to an exchange of the acetone ligand by C_6D_6 (Scheme 1). In contrast, the $[VC_3H_6O_2]^+$ ion of interest formed in the reaction of VO_2^+ with propane does not undergo any ligand exchange in the presence of benzene nor any other reaction. Therefore, structure **1** is excluded safely, and by analogy the structure propanal/VO^+ is considered unlikely. Collision-induced dissociation of $[VC_3H_6O_2]^+$ from propane/VO_2^+ yields the ionic fragments V^+ (20%), VO^+ (50%), VOH^+ (10%), VO_2H^+ (15%), $C_3H_5^+$ (2%), and $C_3H_3^+$ (3%). Within experimental error, identical CID spectra were obtained for the $[VC_3H_6O_2]^+$ ions generated by ion/molecule reactions of VO^+ with *n*-propanol and allyl alcohol. Thus, it is concluded that the product of propane oxidation by VO_2^+ is either a complex of VO^+ with allyl alcohol (structure **2**) or the corresponding C−O insertion species (structure **3**). It is important to note that the mere option to form structures **2** and **3** demonstrates the mechanistic complexity of the propane/VO_2^+ system in that both structures involve at least three different C−H bond activations. This mechanistic richness is a major reason for our reluctance to interpret the product distribution of the labeled propanes by means of kinetic modeling (see above). The reaction of mass-selected $VO_2H_2^+$ with propene provides a reverse entry to the propane/VO_2^+ system. Experimentally, some formation of $[VC_3H_6O_2]^+$ is observed upon interacting mass-selected $VO_2H_2^+$ with propene; yet, the reaction is rather slow and occurs only once in about 20 collisions. Consequently, there must exist some substantial, but yet surmountable kinetic bottleneck between $VO_2H_2^+$ + propene and $[VC_3H_6O_2]^+$ + H_2; we return to this aspect further below.

Butane/VO_2^+. As mentioned above, the products formed in the reaction of *n*-butane with VO_2^+ are again different from those with ethane and propane (Figure 1). More detailed information can be derived from the

(32) Trage, C.; Zummack, W.; Schröder, D.; Schwarz, H. *Angew. Chem.* **2001**, *113*, 2780; *Angew. Chem., Int. Ed.* **2001**, *40*, 2708.
(33) Loos, J.; Schröder, D.; Zummack, W.; Schwarz, H. Thissen, R.; Dutuit, O. *Int. J. Mass Spectrom.* **2002**, *214*, 105.
(34) Trage, C.; Schröder, D.; Schwarz, H. *Organometallics* **2003**, *22*, 693−707.
(35) Schwarz, H. *Top. Curr. Chem.* **1981**, *97*, 1−31.

Table 2. Intensities[a] for the Most Intense Fragmentation Channels of Butane Isotopologs upon Reaction with VO_2^+ (figures calculated for a completely random H/D distribution are given in italics when necessary)

Combined Loss of Dihydrogen and Water

Δm	−20	−21	−22	−23	−24
$CH_3CH_2CH_2CH_3$	100				
$CD_3CH_2CH_2CH_3$	20	70	10		
	17	*50*	*30*	*3*	
$CD_3CD_2CH_2CH_3$[b]	2	28	60	10	
	2	*24*	*48*	*24*	*2*

Loss of Butene[c]

Δm	−56	−57	−58	−59	−60	−61
$CH_3CH_2CH_2CH_3$	100					
$CD_3CH_2CH_2CH_3$			20	80		
$CD_3CD_2CH_2CH_3$				< 1	20	80

Loss of Ethene

Δm	−28	−29	−30	−31	−32
$CH_3CH_2CH_2CH_3$	100				
$CD_3CH_2CH_2CH_3$	60		40		
$CD_3CD_2CH_2CH_3$	60				40

Loss of Methane

Δm	−16	−17	−18	−19	−20
$CH_3CH_2CH_2CH_3$	100				
$CD_3CH_2CH_2CH_3$		40		60	
$CD_3CD_2CH_2CH_3$[b]		40		60	

[a] Observed intensities are ^{13}C-corrected, extrapolated to a reaction time of 0 s to account for H/D exchange occurring with background water, and normalized to $\Sigma = 100$ for each pathway. [b] Spectra obtained in high-resolution mode to distinguish between C_3-, C_4-, and ^{13}C-peaks. [c] See discussion for the other assignments of the neutral molecule lost.

reactions of [1,1,1-D_3]- and [1,1,1,2,2-D_5]-butane (Table 2). In the unlabeled case, a major channel corresponds to C−C bond cleavage leading to $[VC_2H_6O_2]^+$ concomitant with loss of C_2H_4. For both labeled precursors, either only one or all deuterium atoms are found in the ionic product. Therefore, the central C−C bond is broken without occurrence of H/D exchange. This scenario implies that one hydrogen atom from a terminal position is transferred to the metal and remains in the ionic product concomitant with formation of ethene as a neutral product. For both isotopologs, the loss of C_2H_4 prevails over the losses of deuterated ethenes, and the data indicate a kinetic isotope effect of KIE = 1.5 ± 0.2. Further, the resulting $[VC_2H_6O_2]^+$ ion rapidly reacts with water present in the background of the mass spectrometer to form $[VO_3H_4]^+$, i.e., a formal exchange of an ethene ligand against H_2O. Accordingly, the $[VC_2H_6O_2]^+$ ion is tentatively assigned as $(HO)_2V\text{-}(C_2H_4)^+$.

Two minor pathways of C−C bond cleavages lead to the formation of $[VC_3H_6O_2]^+$ and $[VC_3H_4O_2]^+$; thus, ions of the very same elemental compositions as discussed above for the reaction of VO_2^+ with propane. Similar to the loss of ethene, the data in Table 2 clearly demonstrate that C−C bond breaking en route to the loss of methane occurs without H/D exchange. Thus, neutral methane is formed by combination of an intact methyl group with a hydrogen atom from the other methyl group. Accordingly, the formation of methane involves a formal 1,3-elimination rather than a 1,2-elimination pathway, which is common for most other transition metal ions.[29] Again, the branching ratios translate into KIE = 1.5 ± 0.2 for a shift of a hydrogen atom of the methyl groups. Further, a CID spectrum of the $[VC_3H_6O_2]^+$ ion formed after loss of methane closely resembles the one obtained for the corresponding ion generated from propane/VO_2^+. Methane elimination from butane/VO_2^+ may therefore be analogous to the loss of dihydrogen from propane/VO_2^+, yielding the same product ion in both cases.

The situation is markedly different for the two remaining reaction channels, which occur without C−C bond breaking. The formation of $VO_2H_2^+$ seems to be the equivalent to ethene elimination in the reaction of VO_2^+ with ethane.[8] The data for the labeled butanes is in accord with both 1- and 2-butenes being formed as neutral molecules, even though the exact relative isotope distributions might be obscured by fast subsequent H/D exchanges in the reaction of the vanadium dihydroxide cation with background water;[28] therefore, no KIE is explicitly given. Nevertheless, one has to point out that the nature of neutral $[C_4H_8]$ is unknown and it may not necessarily be one molecule only. In fact, from a merely thermochemical point of view, combined losses of either butadiene and dihydrogen or two ethene molecules are conceivable as well.[28] The ionic product of the combined H_2/H_2O loss is intuitively interpreted as a complex of butadiene with the VO^+ cation. The most intense signals obtained when reacting the labeled butanes with VO_2^+ are indeed consistent with this assignment, whereas some minor products suggest either that other isomers (e.g., ketene or alkyne complexes) are produced as well or that partial H/D scrambling is involved. However, formation of ethyl ketene cannot explain 10% of $\Delta m = -22$ for [1,1,1-D_3]-butane, and alkyne formation does not fit the data obtained for [1,1,1,2,2-D_5]-butane. Accordingly, partial H/D atom scrambling seems to best explain the isotope patterns observed experimentally.

All of the minor products formed in the oxidation of isobutane with VO_2^+ can be understood by considering this particular substrate as an intermediate case between propane and *n*-butane. Yet, the major product is again unique in that a hydride is transferred to the vanadium oxide to yield a carbenium ion concomitant with neutral OVOH. The occurrence of this reaction channel precisely for isobutane is easily rationalized by the particular stability of the *tert*-butyl cation which can be formed from this substrate without any complex rearrangements via direct activation of the relatively weak tertiary C−H bond.

Theoretical Results

To gain a better understanding of the remarkable difference in the reactivity of VO_2^+ toward ethane and propane, the potential energy surface for the oxidation of propane by VO_2^+ has been explored using DFT calculations for both the singlet and triplet reaction pathways. The similar theoretical approach in the previous study on the oxidation of ethane by VO_2^+ allows a straightforward comparison with the present results.[8,28,36] The issues addressed in the theoretical

(36) Gracia, L.; Sambrano, J. R.; Safont, V. S.; Calatayud, M.; Beltran, A.; Andres, J. *J. Phys. Chem. A* **2003**, *107*, 3107−3120.

Scheme 2

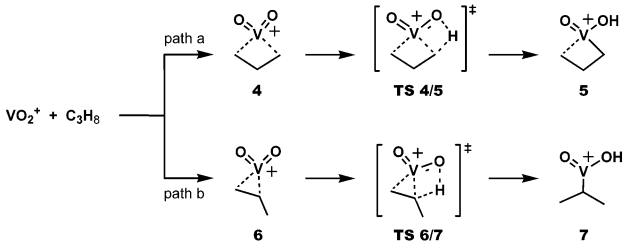

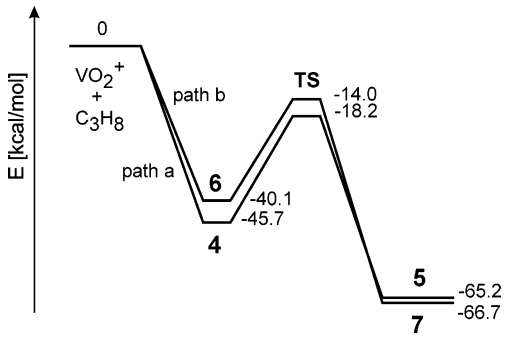

Figure 2. Potential energy diagram for the initial C−H bond activation of propane by VO_2^+ (singlet surface) calculated at the B3LYP/6-311G** level of theory (energies relative to singlet VO_2^+ + propane in kcal/mol).

section are (i) the structure of the product ion $[VC_3H_6O_2]^+$ and (ii) the origin of the different reactivity of VO_2^+ toward ethane and propane.

Despite a huge number of possibilities due to the size and flexibility of the VO_2^+/propane system, we consider structures **1**, **2**, and **3** in Chart 1 as probable product ions on the basis of the discussion in the Experimental Section and therefore concentrate on putative reaction pathways for their formation. Of course, one cannot ensure that these calculations cover all conceivable pathways because in a system of this complexity, there always remains the possibility of other relevant intermediates. All calculated reaction pathways including geometries and relative energies of the minima and transition structures are given in Figures S1−S4 (Supporting Information). Here, we restrict ourselves to the energetically most favorable and therefore presumably most important reaction pathways.

As the very first step of the oxidation of propane by VO_2^+, the reactants come into contact to form one of two possible encounter complexes as shown in Scheme 2. The first one exhibits an η^2-C_3H_8 binding mode with an interaction between the metal ion and the two methyl groups (complex **4**). The other one reveals a different η^2-C_3H_8 binding mode in which the metal ion interacts with a methyl and the central methylene group (complex **6**). These two encounter complexes open up two different reaction channels for propane oxidation. The first one (path a in Scheme 2) finally leads to complexes **2** and **3**, whereas a product ion of structure **1** is generated in path b. In the initial stage of path a, bond activation of complex **4** leads to the *n*-propyl complex $(n\text{-}C_3H_7)V(O)(OH)^+$ **5** via insertion of the metal in a primary C−H bond of propane. In turn, complex **6** enables the activation of a secondary C−H bond (path b), which results in the isopropyl complex $(i\text{-}C_3H_7)V(O)(OH)^+$ **7**. For the following sections it is important to keep in mind that the two reaction channels already separate in the encounter complexes in that the resulting insertion intermediates do not interconvert at later stages.

The singlet ground state of VO_2^+ is 34.7 kcal/mol lower in energy than the nearest triplet state according to the present DFT calculations.[8,36] Therefore, the initial steps of propane oxidation by VO_2^+ proceed on the singlet potential energy surface as shown in Figure 2. In path a, a four-centered transition structure for the cleavage of a primary C−H bond of propane lies 18.2 kcal/mol below the entrance channel of separated propane and VO_2^+. The alternative four-centered transition structure for the activation of a secondary C−H bond of propane (path b) is 4.2 kcal/mol higher in energy. The resulting complexes **5** and **7** formed upon insertion of the metal in the respective C−H bonds are both stabilized by about 65 kcal/mol relative to VO_2^+ + propane. Interestingly, the insertion species **5** bears additional stabilization by an agostic interaction with the terminal methyl group. Accordingly, path a is energetically preferred over path b. As shown below, these two four-centered transition structures are energetically high-lying in comparison to the activation barriers in later stages of the reaction coordinate. Hence, the initial C−H bond activations are expected to act as mechanistic distributors for the various pathways in the oxidation of propane by VO_2^+.

Let us begin with the discussion of the subsequent steps with the initial activation of a primary C−H bond along path a. In the *n*-propyl complex **5**, there are two possibilities to continue by breaking the second C−H bond as indicated in Scheme 3: either activation of a secondary C−H bond takes place (path a1, a formal 1,2-elimination) or a cleavage of a primary C−H bond of the methyl group occurs (path a2, a formal 1,3-elimination). A simplified, combined energy diagram for paths a1 and a2 in the singlet and triplet state is depicted in Figure 3; optimized geometries of the reaction intermediates and transition structures are given in Figure 4.

Following path a1, the formal 1,2-elimination via the four-centered transition structure **TS 5/8** leads directly to the propene complex $(C_3H_6)V(OH)_2^+$ **8**, which appears

Scheme 3

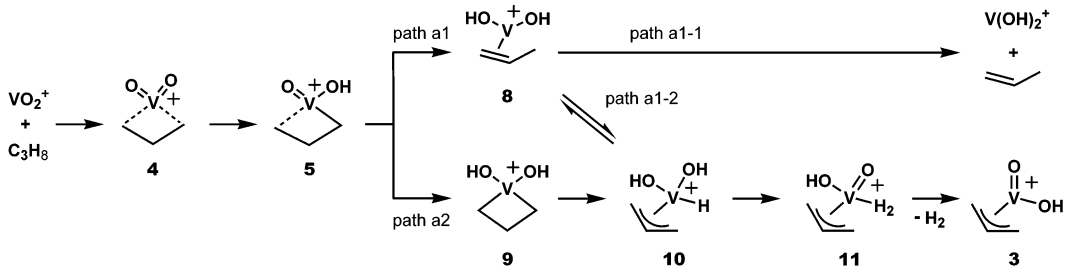

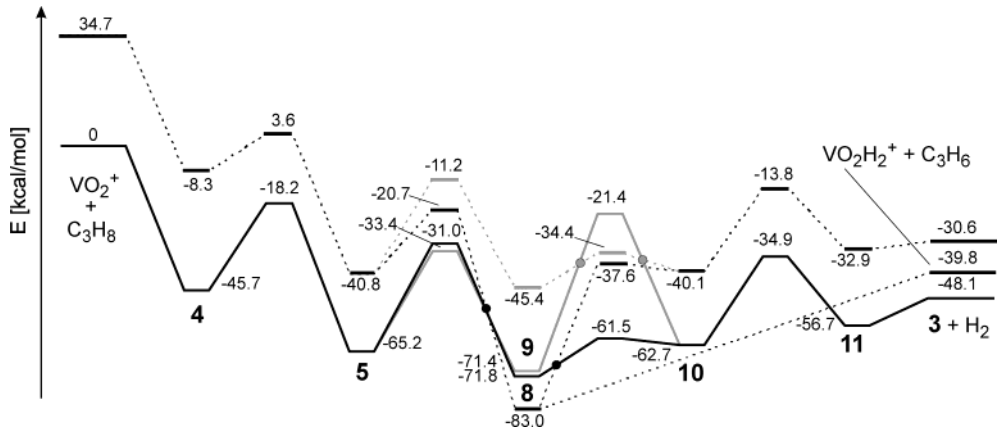

Figure 3. Potential energy diagram for the most probable reaction pathways after initial activation of a primary C−H bond in the reaction of VO_2^+ with propane calculated at the B3LYP/6-311G** level of theory (energies relative to singlet VO_2^+ + propane in kcal/mol). Black lines: path (a1); gray lines: path a2; solid lines: singlet surface; dashed lines: triplet surface. A solid circle stands for a crossing point of the singlet and triplet surfaces.

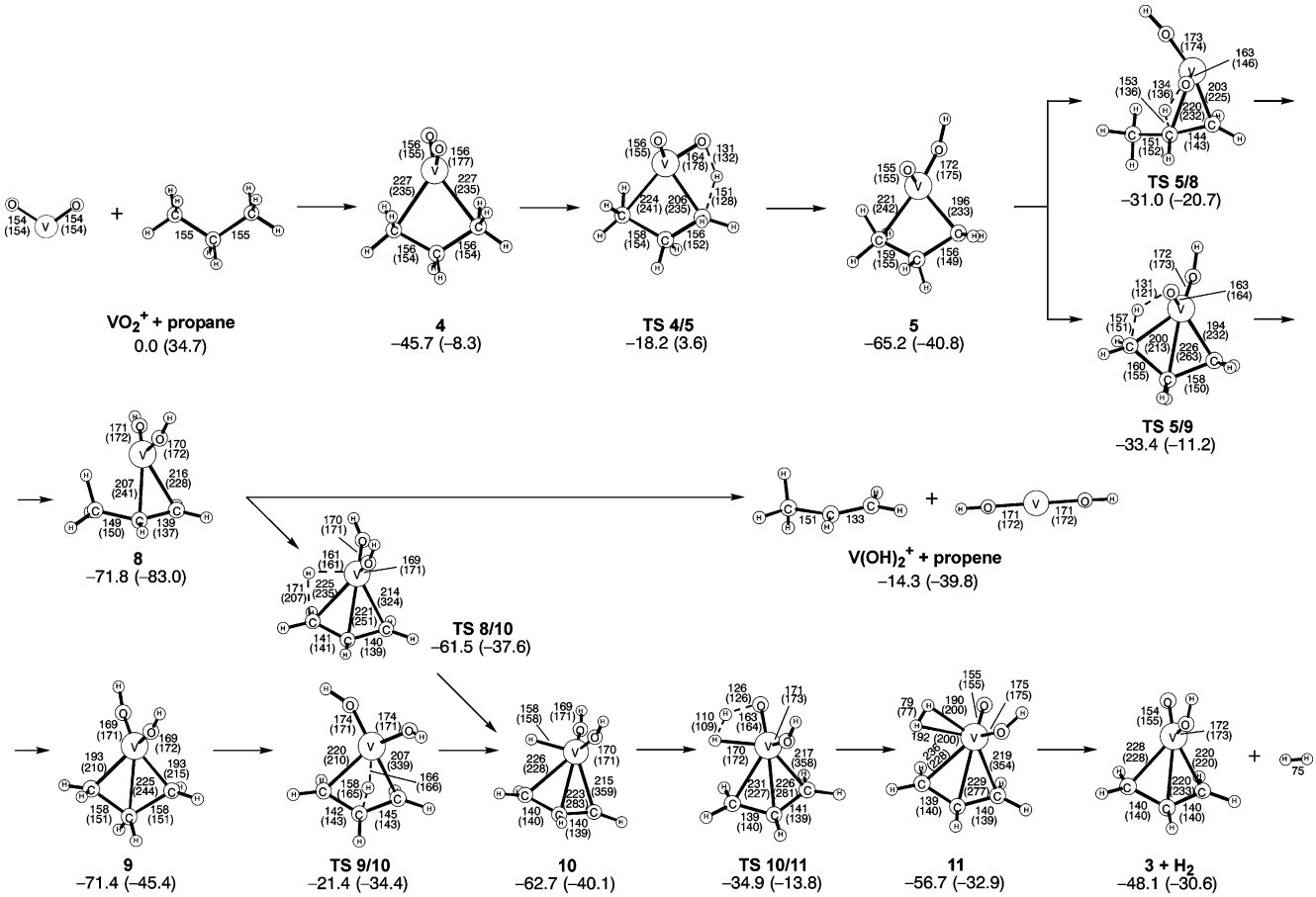

Figure 4. Geometries of the stationary points on the most probable reaction pathways after initial activation of a primary C−H bond in the reaction of VO_2^+ with propane calculated at the B3LYP/6-311G** level of theory (energies relative to singlet VO_2^+ + propane in kcal/mol; bond lengths in pm). The given numbers refer to the singlet surface, numbers in brackets to the triplet surface.

to be the global minimum of the propane/VO_2^+ system according to the present DFT calculations. Complex **8** is the only species in the entire system studied with a triplet ground state that is 11.2 kcal/mol more stable than the corresponding singlet. As shown in Figure 3, the two potential energy surfaces cross between the four-centered transition structure and **8**. Accordingly, both singlet and triplet potential energy surfaces are relevant for the reactions evolving from **TS 5/8**, whereas the initial C−H bond activations exclusively involve the singlet surface. Complex **8** is another branching point, where two more reaction channels are accessible, i.e., paths a1-1 and a1-2, as indicated in Scheme 3. Path a1-1 leads directly to $V(OH)_2^+$ and propene; the overall reaction along this pathway thus is analogous to the reaction of VO_2^+ with ethane.[8] The dissociation limit toward $V(OH)_2^+$ + propene in the triplet state lies 39.8 kcal/mol below the entrance channel VO_2^+ + propane. Therefore, the reaction along path a1-1 is expected to proceed rapidly, provided that the required spin change

from the singlet to the triplet surface can take place. Alternatively, path a1-2 can yield the singlet complex $(C_3H_5)V(O)(OH)^+$ **3** and H_2. This reaction channel is initiated by a β-hydrogen transfer in complex **8** proceeding via a three-centered transition structure **TS 8/10** to form the allyl complex **10**. **TS 8/10** and complex **10** in the singlet state are 23.9 and 22.6 kcal/mol more stable than in the triplet state, respectively. Hence, β-hydrogen transfer can effectively proceed on the singlet potential energy surface. Because **10** lies energetically close to **TS 8/10**, hydrogen transfer should be reversible to yield again the propene/$V(OH)_2^+$ complex **8**. After formation of **10**, a hydrogen atom from one of the hydroxy groups can combine with the hydride via **TS 10/11** to eliminate an H_2 molecule. This viable exit channel of the propane/VO_2^+ system results in a $[VC_3H_6O_2]^+$ complex with structure **3**. Both dissociation channels are energetically comparable, yet, path a1-1 is expected to be favored over path a1-2 as far as entropy is concerned (direct dissociation vs rearrangement). Nevertheless, the conversion into $V(OH)_2^+$ + propene from complex **8** along path a1-1 can proceed efficiently only on the triplet surface, whereas path a1-2 to afford **3** + H_2 can reside on the singlet potential energy surface. The branching ratio is therefore expected to be determined by the probability of spin inversion. If spin interconversion is facile, propene elimination is expected to prevail, whereas dehydrogenation can compete if the system stays on the singlet surface. Therefore, the switch between the spin states should control the outcome of the oxidation of propane by VO_2^+ along path a1.[37]

In path a2, γ-C−H bond activation in complex **5** leads to the formation of the quite stable species **9**, which can be classified as a vanadacyclobutane derivative. Afterward, **9** is converted into complex **10** via a three-centered transition structure for a β-hydrogen transfer. If spin inversion is slow, this conversion can also occur on the corresponding singlet surface, which lies 13 kcal/mol higher in energy than the triplet surface. However, the β-hydrogen transfer over a four-membered ring in the singlet state needs about as much energy as the initial activation of a C−H bond of propane, thus constituting the rate-determining step of the overall reaction. Moreover, **TS 9/10** is 12 kcal/mol higher in energy than **TS 5/9** associated with a formal 1,3-elimination such that the reaction back to the *n*-propyl complex **5** can compete. On the triplet surface, the transition structure for the β-hydrogen transfer is lower in energy because the four-membered ring is opened to a σ-allyl-like structure without interaction of the vanadium center with one methylene group; therefore, release of strain energy stabilizes the transition structure with respect to the preceding minimum. However, path a2 on both the singlet and triplet potential energy surfaces is energetically disfavored compared to path a1; see Figure 3. As path a2 offers a more simple access to structure **10**, the final steps of this path are identical to the ones of path a1. The above discussion of the differentiation between the two possible exit channels is thus valid for the entire path a and thereby covers all steps occurring after initial activation of a primary C−H bond.

(37) Poli, R.; Harvey, J. N. *Chem. Soc. Rev.* **2003**, *32*, 1−8.

Scheme 4

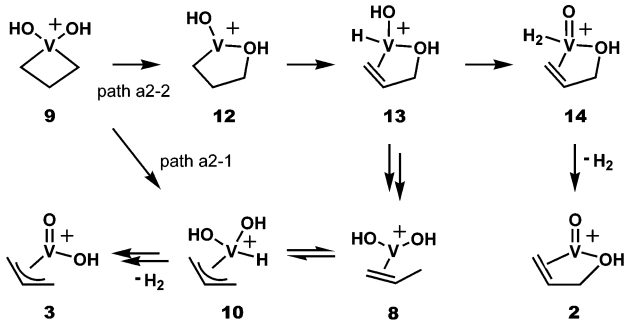

In the last part of the discussion of the primary C−H bond activation, let us pay some attention to possible reaction pathways in which structure **2** with an intact C−OH bond is formed as the product ion in the oxidation of propane by VO_2^+. Yet, all routes leading to complex **2** are energetically less favored compared to the ones leading to the allyl complex **3**. As all details are given in Figures S1 and S2, here we will comment only briefly on the results obtained in this respect. A transfer of the OH group from the metal back to the carbon chain in complex **9** (path a2-2, Scheme 4) is the most promising route for the formation of **2**. The vanadacyclobutane **9** can be converted to complex **12** via a three-centered transition structure in which one of the OH groups migrates toward an adjacent methylene group. This transition structure is located 10.5 kcal/mol (singlet state) and 27.0 kcal/mol (triplet state) below the entrance channel VO_2^+ + propane. Accordingly, route a2-2 is at least 10 kcal/mol more energy-demanding than path a2-1 via **TS 9/10** (see above). Once **12** is generated, one of the central C−H bonds can be broken via a three-centered transition structure to form the $(C_3H_5OH)V(H)(OH)^+$ complex **13**. The latter serves as a direct precursor for loss of H_2 via **TS 13/14** associated with the combination of the hydride attached to the metal and the H atom of the hydroxy group. The computed energy of **TS 13/14** is −11.5 kcal/mol for the singlet state and −16.7 kcal/mol for the triplet state relative to the entrance channel VO_2^+ + propane. This is even higher than the initial C−H bond activation of propane in the very beginning of the reaction. Furthermore, another route leading from complex **13** back to the propene complex **8** needs about 20 kcal/mol less energy on both the singlet and triplet surface (see Figures S1 and S2 for details). Therefore, the formation of structure **2** as the product ion in the propane/VO_2^+ system is energetically possible, but very much disfavored in comparison to structure **3**.

Let us now return to the reaction pathways for the formation of the acetone complex **1**, which is straightforward after the cleavage of a secondary C−H bond of propane (path b in Scheme 1). Figure 5 shows the computed energy diagram for the energetically most favored pathway found (singlet and triplet surfaces), and Figure 6 depicts the optimized geometries for the reaction intermediates and transition structures. After the isopropyl complex **7** is formed, rotation of the metal oxide part initiates an insertion of the oxygen atom into the V−C bond concomitant with a switch to the triplet potential energy surface, resulting in the hydroxovanadium alkoxide complex **15** as indicated in Scheme 5. The remaining hydrogen of the central carbon atom is then

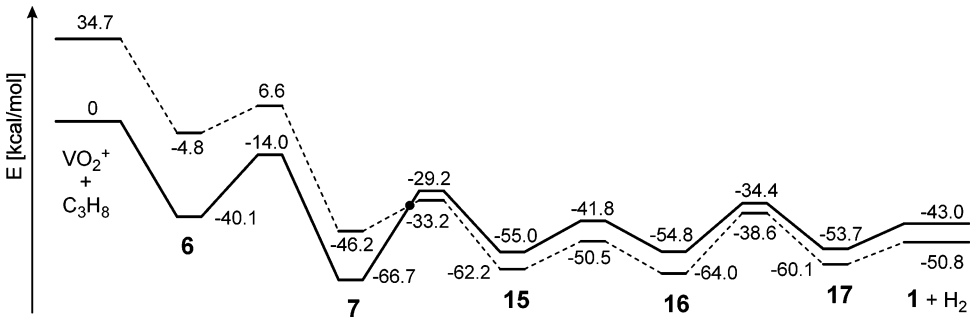

Figure 5. Potential energy diagram for the most probable reaction pathway after initial activation of a secondary C−H bond in the reaction of VO_2^+ with propane calculated at the B3LYP/6-311G** level of theory (energies relative to singlet VO_2^+ + propane in kcal/mol). Solid line: singlet surface; dashed line: triplet surface. A solid circle stands for a crossing point of the singlet and triplet surfaces.

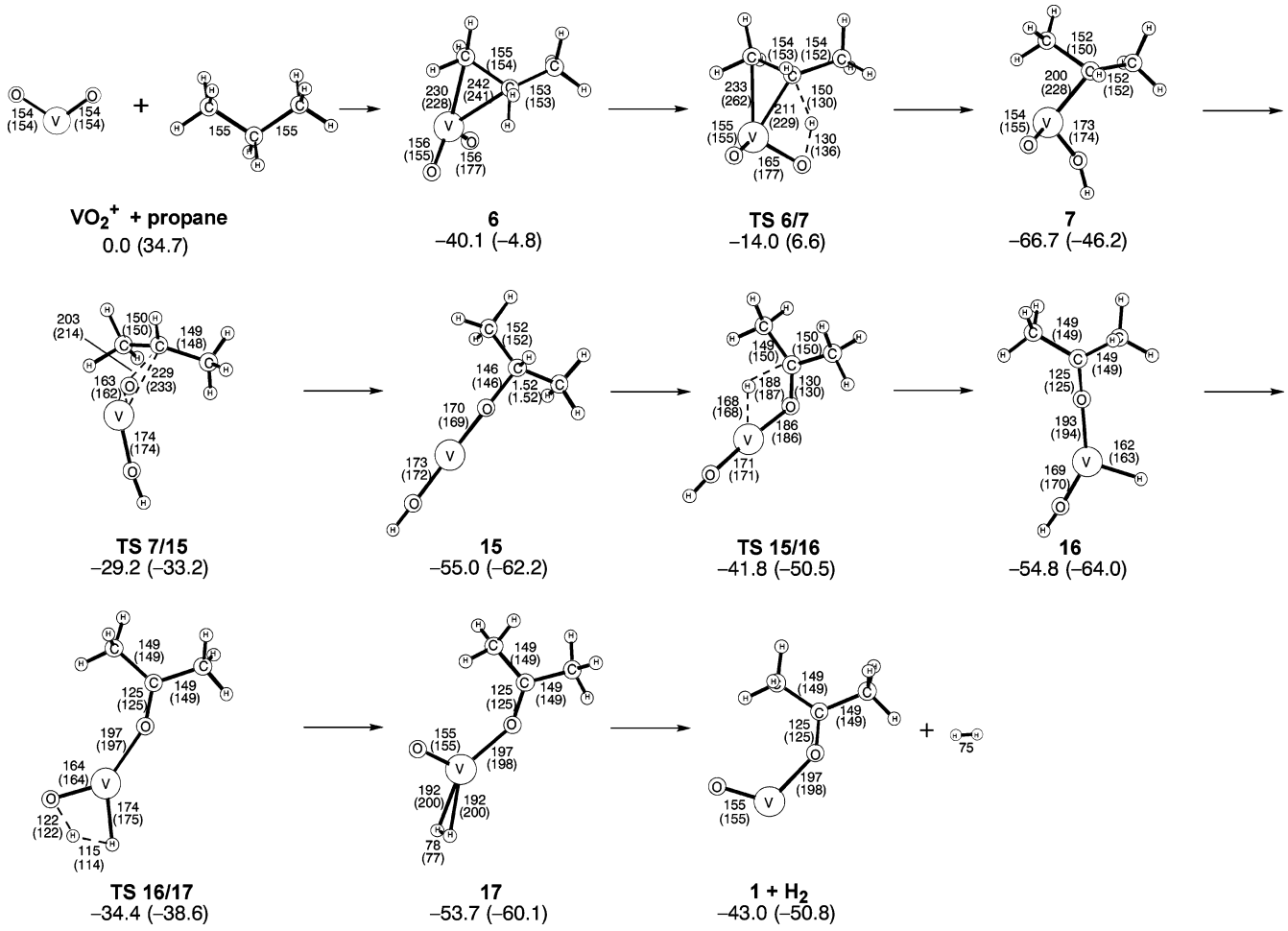

Figure 6. Geometries of the stationary points on the most probable reaction pathway after initial activation of a secondary C−H bond in the reaction of VO_2^+ with propane calculated at the B3LYP/6-311G** level of theory (energies relative to singlet VO_2^+ + propane in kcal/mol; bond lengths in pm). The given numbers refer to the singlet surface, numbers in brackets to the triplet surface.

Scheme 5

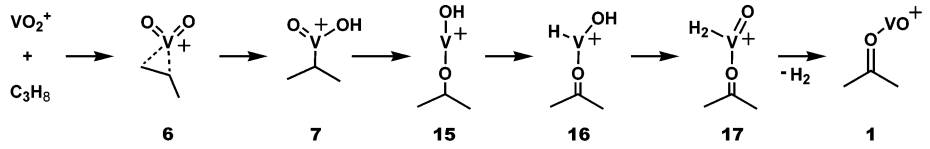

transferred to the metal and can form molecular hydrogen by combination with the hydrogen atom of the hydroxy group. In this route, vanadium ends up in the oxidation state of V^{III}, which is certainly more favorable than reductive elimination of water to (acetone)V^+ with a formal V^I. According to this scenario, no H/D scrambling should occur in the reactions of deuterium-labeled propanes. Some other possibilities leading to the same final product, but differing in the order of insertion and hydrogen shift or in a transfer of the OH group instead

of the oxo group in the initial phase, were studied as well (see Figures S3 and S4 for details). However, these pathways cannot compete with the one described in Figure 5, because at least one transition structure has an energy similar to the entrance channel. Therefore, the initial activation of a secondary C−H bond is followed by yet another activation of the C(2) position, resulting in a formal 1,1-elimination to form the acetone complex **1**. In summary, the generation of the acetone complex **1** is energetically possible via a secondary C−H bond activation (path b), but cannot efficiently compete with path a, because the rate-determining step of the overall oxidation reaction is the initial C−H bond activation in propane. As the **TS 4/5** for the activation of a terminal C−H bond is lower in energy than **TS 6/7** for the activation of an internal one (Figure 2), the former is expected to be favored kinetically, thereby resulting in a discrimination of acetone formation.

Discussion

In conjunction with the theoretical results on propane/VO_2^+, the experimental findings and the implications of the labeling studies allow more concise considerations about the reactions of VO_2^+ with small alkanes, particularly with respect to the experimentally observed drastic changes in the product patterns.

Propane/VO_2^+. First of all, a comparison of the experimental and theoretical results about the structure of the $[VC_3H_6O_2]^+$ ion formed in the reaction of VO_2^+ with propane shows nice agreement in the assignment of this ionic product to structure **3**, that is the allyl complex $(C_3H_5)V(O)(OH)^+$. The intuitively expected ketone complex **1** is not observed. Particularly notable in this reaction is the fact that activation of primary C−H bonds is preferred. This behavior is not only counterintuitive but also in marked contrast to the reactions of most other transition metal fragments in the gas phase.[29,38] The present theoretical studies provide a rationale for this behavior in that the encounter complex in which the VO_2^+ cation interacts with both terminal methyl groups is considerably more stable than the one with a coordination mode involving the central methylene group of propane. The very same applies for the corresponding transition structures of the rate-determining C−H bond activations. Thereby, theory also explains the practical absence of the (acetone)VO^+ complex **1** as a dehydrogenation product. Note that the various equilibrations, which are accessible prior to dissociation, may also account for some of the H/D scrambling observed in the experiments. It is obvious from both experiment and theory, however, that what seems to be a simple reaction (dehydrogenation of propene) turns out as a rather complex process with many different minima and transition structures involved. Thus, even with the data for seven different isotopologs of propane, the experimentally observed product distributions cannot be modeled kinetically due to an underdetermined system of coupled differential equations. Specifically, kinetic modeling with inclusion of competing 1,2- and 1,3-dehydrogenations as well as partial H/D equilibration reproduces the experimentally observed isotope patterns only when inverse KIEs are allowed. The latter option resembles opening Pandora's box, however, because once a hidden hydrogen transfer is involved, sequences of similar processes may occur as well such that the number of variables exceeds that of the independent observables.

Even more subtle is the answer to the question about the origin of the different product distributions for ethane and propane. In the case of ethane, formation of $V(OH)_2^+$ and neutral ethene is the only product channel accessible energetically.[8] In contrast, a third hydrogen transfer is possible in the propane case, thereby opening up new reaction channels. On the basis of the calculations for the reaction of VO_2^+ with propane, one would expect that a mixture of $V(OH)_2^+$ and $[VC_3H_6O_2]^+$ is formed as the ionic products, where the former is assumed to predominate due to its easier accessibility from the reactants and the similar energy demand as the dehydrogenation channel. In the experiment, however, dehydrogenation to afford $[VC_3H_6O_2]^+$ is observed almost exclusively. As indicated above, spin restrictions could explain the obvious discrepancy. If spin inversion is slow, elimination of propene to afford $V(OH)_2^+$ in its triplet ground state is disfavored, and hence the $[VC_3H_6O_2]^+$ ion with structure **3** should be formed. Only if spin inversion were efficient would $V(OH)_2^+$ be expected as a major product. The reverse approach to the propane/VO_2^+ system via propene/$VO_2H_2^+$ provides further insight in this respect. Thus, dehydrogenation to afford $[VC_3H_6O_2]^+$ is observed with an efficiency of only about 5% compared to the collision rate. This moderate rate is fully consistent with both the change in spin multiplicity from triplet $V(OH)_2^+$ to singlet $(C_3H_5)VO(OH)^+$ and the location of **TS 10/11** slightly above the $V(OH)_2^+ + C_3H_6$ entrance channel. In summary, these considerations imply that spin change is possible in the propane/VO_2^+ system. However, once the insertion intermediate **5** is formed, the further path to products is located much below the preceding rate-determining step and is therefore expected to proceed rather fast. As a consequence, spin inversion to the triplet surface may no longer be able to compete with dehydrogenation to finally afford singlet $[VC_3H_6O_2]^+$. In the case of ethane, however, there simply is no possibility to avoid a spin change from the singlet to the triplet surface, because both loss of ethene to afford $V(OH)_2^+$ and dehydrogenation to form a $(CH_3CHO)VO^+$ complex terminate on the triplet surface. Thereby, the theoretical results provide a conceptual rationale for the different reactivity patterns for ethane and propane in which spin inversion acts as a decisive factor.[39] For vanadium as an early 3d element, not only are high valences common, such as formal V^V in structure **3**, but also spin inversion may be slow enough for small compounds in the gas phase.[40] Note, however, that it is not the bond-activation phase that is influenced by spin restrictions, but the product distribution in the subsequent steps.

(38) For another example of 1,*n*-elimination of H_2 ($n \geq 3$), see: Kang, H.; Beauchamp, J. L. *J. Am. Chem. Soc.* **1986**, *108*, 7502−7509.

(39) Schröder, D.; Shaik, S.; Schwarz, H. *Acc. Chem. Res.* **2000**, *33*, 139−145.

(40) Rue, C.; Armentrout, P. B.; Kretzschmar, I.; Schröder, D.; Harvey, J. N.; Schwarz, H. *J. Chem. Phys.* **1999**, *110*, 7858.

(41) Efficiency relative to the gas-kinetic collision rate calculated according to: Su, T. *J. Chem. Phys.* **1988**, *89*, 5355−5356.

Scheme 6

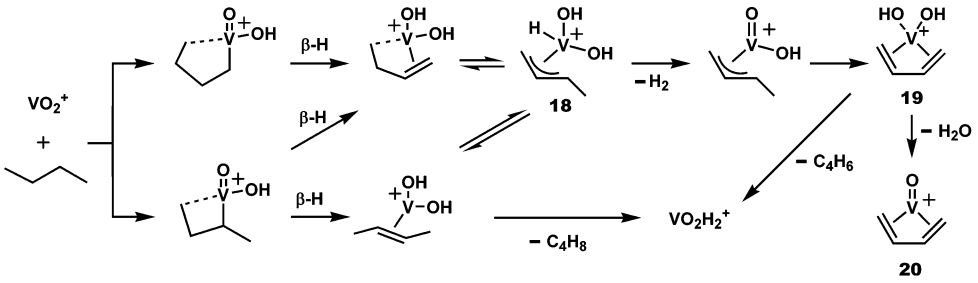

Butane/VO_2^+. The above discussion of the ethane/VO_2^+ and propane/VO_2^+ systems demonstrates how misleading simple extrapolations in a homologous row may be. Nevertheless, having achieved some improved mechanistic insight, let us attempt to translate the results obtained by studying the mechanism for propane to the butane/VO_2^+ system with an emphasis on the dehydrogenation mechanism. By analogy with propane, one could assume formation of a similar allyl complex **18** as a key intermediate en route to dehydrogenation, where the only difference is an additional methyl substituent (Scheme 6). In contrast to propane, however, the reaction must not stop after dehydrogenation, but can continue via yet a further H-abstraction from the additional methyl group, eventually leading to (butadiene)$V(OH)_2^+$, **19**. Then, loss of either butadiene or water can take place, where the latter (**19** → **20**) is more probable than in the ethane/VO_2^+ and propane/VO_2^+ systems. Thus, the combined eliminations of H_2 and H_2O are not observed for ethane and propane because the intermediates formed do not bear activated C−H bonds. We note in passing that the $V(OH)_2^+$ product could be formed also directly upon loss of butene, a reaction channel that may be disfavored for similar reasons as discussed for the propane case. Nevertheless, the elemental formula $[C_4H_8]$ for the neutral molecule(s) lost upon formation of $V(OH)_2^+$ may stand for a mixture of butenes, butadiene, and dihydrogen, or two molecules of ethene. Finally, the partial H/D equilibration observed in the $H_2 + H_2O$ pathway does not find a match in the C−C cleavage products. This result strongly suggests that C−H and C−C bond activations are uncoupled from each other in that the initial bond-activation steps are quasi-irreversible and determine the fate of the intermediates. The latter conclusion is in nice agreement with the rate-determining character of the initial C−H bond activations in the propane/VO_2^+ system.

Conclusion

Whereas the VO_2^+ cation reacts with ethane by elimination of ethene, the corresponding reaction with propane almost exclusively leads to dehydrogenation. The difference in reactivity can be ascribed to the formation of the allyl complex $(C_3H_5)V(O)(OH)^+$ after loss of H_2, which provides a new and strongly favored reaction channel that is impossible in the case of ethane. The analysis of mass spectrometric experiments including various labeling studies is very much assisted by theoretical investigations of the propane/VO_2^+ system using DFT. In fact, the calculated potential energy surface elucidates some of the mechanistic intricacies of propane dehydrogenation. The pronounced difference in product distribution compared to ethane, however, needs consideration of spin multiplicity as an additional factor. The results can further be used to delineate a first picture for the C−H bond activations observed in the reaction of butane with the VO_2^+ cation.

Acknowledgment. Financial support by the Deutsche Forschungsgemeinschaft (SFB 546) and the Fonds der Chemischen Industrie is acknowledged. Further, we thank the Konrad-Zuse Zentrum Berlin for generous allocation of computer time. K.Y. acknowledges the Ministry of Culture, Sports, Science and Technology of Japan, Japan Society for the Promotion of Science, the Takeda Science Foundation, and Kyushu University P & P "Green Chemistry" for their support of this work. T.Y. thanks Japan Society for the Promotion of Science for a graduate fellowship. Computations were in part carried out at the Computer Center of the Institute for Molecular Science. The authors appreciate helpful comments by Dr. J. N. Harvey and thank Dr. M. Pykavy for an insightful analysis of the wave function of the $V(OH)_2^+$ cation.

Supporting Information Available: Relative energies and geometries (bond lengths) of all stationary points localized in the calculations are summarized in Figures S1, S2, S3, and S4. This material is available free of charge via the Internet at http://pubs.acs.org.

OM030353H